

05,13

Magnetic sensor based on spin waves

© A.V. Kozhevnikov¹, S.L. Vysotskii^{1,2,*}, G.M. Dudko¹, Yu.V. Khivintsev¹, Yu.V. Nikulin¹, Yu.A. Filimonov^{1,2}

¹ Saratov Branch, Kotelnikov Institute of Radio Engineering and Electronics, Russian Academy of Sciences, Saratov, Russia

² Chernyshevsky Saratov National Research State University, Saratov, Russia

* E-mail: vysotsl@gmail.com

Received April 29, 2022

Revised April 29, 2022

Accepted May 12, 2022

The spectrum of spin waves (SW) of tangentially magnetized films of yttrium iron garnet (YIG) with a surface metastructure in the form of gratings of etched grooves with a period Λ close to the film thickness d ($\Lambda \sim d$) has been experimentally and numerically studied. It has been found that the spectrum of the signal reflected from a microstrip transducer with a width $w \gg d, \Lambda$ located on the YIG film contains absorption lines associated with the excitation of the SW of the surface metastructure. In the case when the magnetic field H and the transducer are oriented along the grooves, the absorption lines of the metastructure are located at frequencies f^* near the short-wavelength edge of the spectrum of the surface magnetostatic (Damon–Eshbach) wave f_s . It is shown that f^* linearly depends on H , which can be used to develop magnetic field sensors. The results of measurements of dependences $f^*(H)$ are in qualitative agreement with the results of micromagnetic modeling.

Keywords: magnetostatic waves, one-dimensional grating, surface structure, sensor of magnetic field.

DOI: 10.21883/PSS.2022.09.54157.05HH

1. Introduction

Interest in the study of spin waves in magnetic periodic structures (magnonic crystals) is associated with the study of the features of the spectrum formation of spin-wave excitations due to the nonuniformity of the ground state, the dependence of the forbidden band width in the spectrum of spin waves on the geometric and magnetic parameters of the periodic structure, the presence of structural defects, as well as the dependence of the spectrum formation conditions on the ratio of the contributions of the dipole-dipole and exchange interactions [1–8].

In addition to the fundamental interest in their properties, magnonic crystals (MC) can be used to develop UHF information processing devices [9–12], as well as, for example, to create magnetic sensors [13–17]. In the latter case, the effect of the forbidden band formation at the Bragg resonance frequency in the spectrum of spin waves propagating in MC, and the dependence of the resonance frequency of this band on the magnitude of the bias field are used.

Note that most often in experimental studies of the MC properties at UHF the yttrium iron garnet (YIG) films are used, on the surface of which, using precision etching [11,18,19] or periodic metallization [13,15] a one-dimensional or two-dimensional periodic structure is formed. The emphasis in MC studies is on studying the parameters of the Bragg stopbands in the frequency dependences of the transmission coefficient of propagating spin waves, while the value Λ is chosen from the condition $\Lambda > \lambda_{\min}$, where λ_{\min} is the minimum wavelength observed

in the SW experiment. When the period of the surface structure decreases to $\Lambda < \lambda_{\min}$, it becomes subwave (with respect to propagating SW) and can be interpreted as a two-dimensional analogue of a metamaterial — a metasurface [20,21]. The SW propagation in YIG films with a metasurface has a number of features in comparison with both a flat film and with a MC [20,21].

The purpose of this paper is to study the features of the spectrum of YIG films with a surface metastructure associated with the presence of intrinsic excitations of the metasurface and to identify the prospects for making magnetic field sensors based on them.

2. Experimental samples, experiment procedure and measurement results

For the samples preparation a YIG film epitaxially grown on a substrate of gadolinium-gallium garnet 0.5 mm thick with crystallographic orientation (111) with thickness $d = 7.7 \mu\text{m}$, saturation magnetization $4\pi M = 1750 \text{ G}$ was used. To form surface gratings from grooves, photolithography and ion etching technologies were used. At that due to the low selectivity of etching, the groove profiles noticeably differ from the rectangular one. The Table shows the parameters of several studied samples (see also inset a to Fig. 1).

To study the spectrum of intrinsic excitation we used an approach similar to [22]. The samples were placed on a microstrip antenna $w = 50 \mu\text{m}$ wide so that the grooves were oriented along the antenna, and were magnetized

Parameters of several studied samples

N ^o	Λ , μm	a , μm	b , μm	h , μm
1	8	3	5	0.9
2	6	2	3	1
3	5	0	2	1.1

in the plane of the YIG film parallel to the antenna. UHF power was applied to the antenna from the Agilent E5071C-480 network analyzer. The frequency dependence of the power $S_{11}(f)$ reflected from the antenna on the bias field H was studied.

In Fig. 1 curve 1 corresponds to $S_{11}(f)$ for sample N^o 1 at $H = 760$ Oe. $S_{11}(f)$ decreasing in the frequency range, indicated in Fig. 1 as MSSW (magnetostatic surface waves), corresponds to the excitation of a surface magnetostatic wave (MSSW). The lower frequency limit of the interval corresponds to the long-wavelength limit of the MSSW spectrum $f_0 = \sqrt{f_H \cdot (f_H + f_m)}$, while the upper one $f_{\lambda_{\min}}$ is determined from dispersion equation [23]:

$$f_-^2 = f_0^2 + \frac{f_m^2}{4} (1 - e^{-2kd}), \quad (1)$$

$f_H = \gamma H$, $f_m = \gamma 4\pi M$, k is MSSW wave vector, $\gamma \approx 2.8$ MHz/Oe is gyromagnetic ratio in YIG, at the value $k = \pi/w$ corresponding to the minimum wavelength of the MSSW excited by the antenna width w . Besides, in the dependence $S_{11}(f)$, an asterisk marks a narrow-band dip with a central frequency f^* , which turned out to be close to the upper frequency boundary of the region of existence of MSSW $f_n = f_H + f_m/2$ [23]. The films without the surface metastructure have no such dip. This feature was

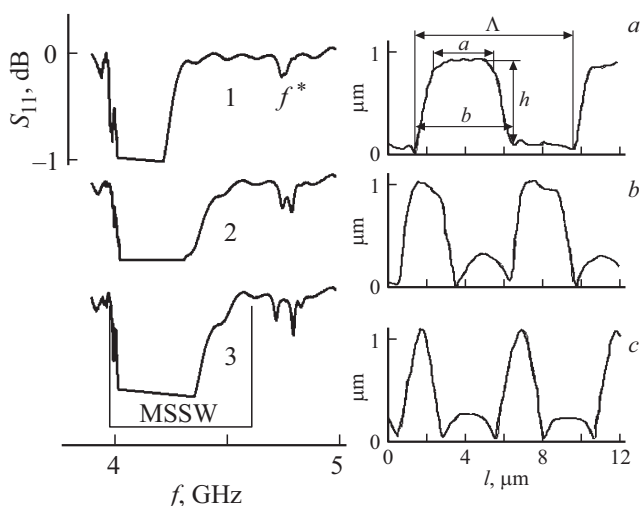


Figure 1. Type of dependencies $S_{11}(f)$ for samples N^o 1, 2 and 3 (see Table) at $H = 760$ Oe. The numbers next to the curves correspond to the numbers of the samples. The vertical scale is the same for all curves. Insets *a–c* show the surface structure profiles obtained using a scanning probe microscope for samples N^o 1, 2, and 3, respectively.

observed for all the studied samples, and the dip could show a „neck“ (curve 2) or split into two separate absorption peaks (curve 3). From a comparison of the profiles of the samples obtained using a scanning probe microscope and the form of dependences $S_{11}(f)$ we can conclude that the more the shape of the protrusion deviates from rectangular towards triangular, the more pronounced is the dip division into two individual peaks. It turned out that the central frequency of a single peak f^* (or the frequencies of two separate peaks) depends linearly on the magnitude of the bias field. For example, in Fig. 2, *a* the dependence $f^*(H)$ in the interval H from 1 Oe to 1.7 kOe is represented by line *I*.

We measured the dependence $S_{11}(f)$ under conditions when the groove axis deviated from the direction of the field H . In Fig. 3, *a* curves 1 and 2 represent these dependences obtained at $H = 47$ Oe for $\varphi = 0$ (curve 1) and $\varphi = 20^\circ$ (curve 2), where φ is the angle between the groove axis of the surface structure and the direction of the bias field. It can be seen that as the angle φ increases, the characteristic frequencies of the studied dips decrease, which is typical for the behavior of the short-wavelength edge of the MSSW spectrum.

3. Results of micromagnetic modeling

Using micromagnetic modeling with the OOMMF package [24] and data processing with the Semargl program [25], the spectra of relaxation oscillations in smooth YIG films and subwavelength gratings with parameters corresponding to the experimentally studied structures were obtained. When modeling, the step of the lattice cell in the section (0XZ) of the structure perpendicular to the direction of the microstrips was 50×50 nm, and in the direction (0Y) along the microstrips — one cell in 1 cm (analogous of two-dimensional geometry) was taken. In the direction (0X) the periodic boundary conditions were applied.

Fig. 2, *b* shows the results of modeling the spectra of relaxation oscillations in smooth YIG films (curve 1) and subwavelength gratings (curve 2) with a period of $8 \mu\text{m}$, groove width and depth 4 and $1 \mu\text{m}$, respectively, at $H = 760$ Oe. It can be seen that in both cases the spectra exhibit a peak at a frequency f_0 corresponding to a quasi-homogeneous resonance, and in the presence of a surface structure two more isolated peaks appear at frequencies f_1 and f_2 marked in Fig. 2, *b* *A* and *B*. In Fig. 2, *a* the lines *A* and *B* show the calculated dependencies of f_1 and f_2 on H . It can be seen that the plots of the dependences $f_1(H)$ and $f_2(H)$ are straight lines with slightly different angles of inclination to the abscissa axis, while the calculated frequencies f_1 and f_2 are close to the experimentally measured f^* .

Fig. 3, *b* shows the results of modeling the spectra of relaxation oscillations in the YIG film with a surface metastructure obtained at $H = 10$ Oe for $\varphi = 0, 5^\circ$ and 10° (curves 1, 2 and 3 respectively). It can be seen that as the angle φ increases, the characteristic frequencies of

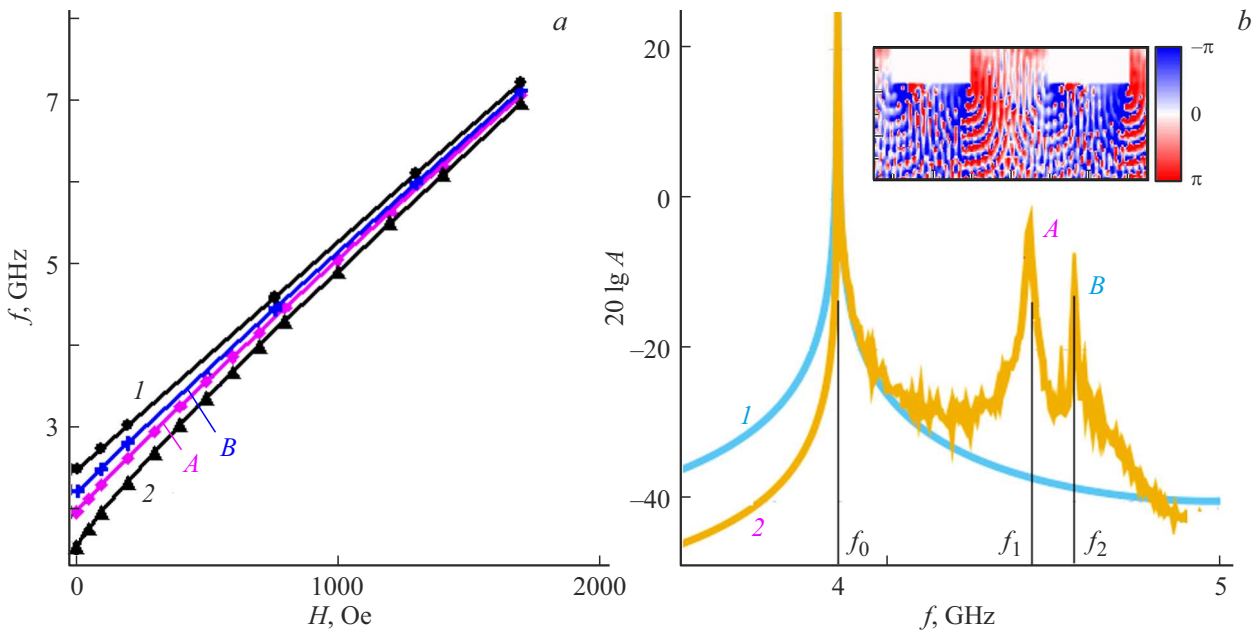


Figure 2. *a*) Dependence on value H of experimentally measured frequency f^* (line 1), calculated frequencies f_1 and f_2 (lines A and B), and the calculated Bragg resonance frequency at $\Lambda = 100\mu\text{m}$ (line 2). *b*) Frequency dependence of the Fourier-amplitude spectral density for the cases of MSSW in the YIG film (curve 1) and in the YIG film with a subwavelength surface structure (curve 2). $H = 760$ Oe. The inset shows a fragment of the phase distribution of the spin excitations calculated for the frequency $f_1 = 4.44$ GHz, which corresponds to the peak A maximum.

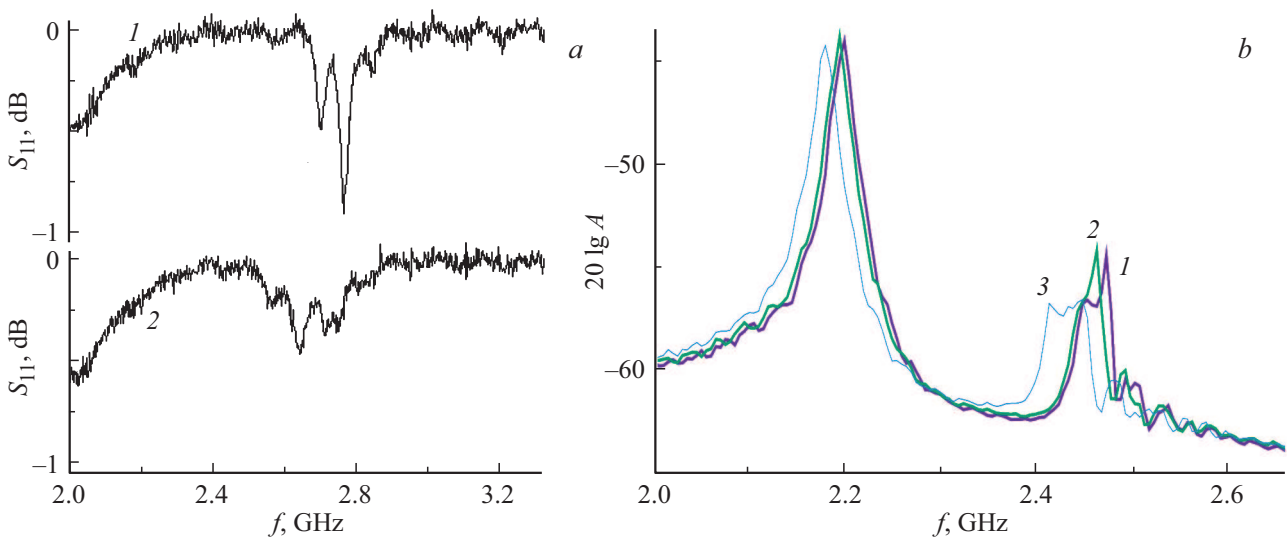


Figure 3. *a*) Dependence $S_{11}(f)$ for sample № 2 at $\varphi = 0$ (curve 1) and 20° (curve 2), $H = 47$ Oe. *b*) Frequency dependence of the Fourier-amplitude spectral density for the cases of SMSW propagation in the YIG film with a subwavelength surface structure at $\varphi = 0, 5^\circ$ and 10° (curves 1, 2 and 3 respectively). $H = 10$ Oe.

the studied dips decrease, which qualitatively agrees with the experimental results.

The inset to Fig. 2, *b* shows a fragment of the phase distribution of the spin excitations over the cross section of the structure calculated for the frequency of 4.44 GHz, which corresponds to the peak maximum A. The calculation was carried out for $\Lambda = 8\mu\text{m}$, $a = 4\mu\text{m}$, $b = 4\mu\text{m}$, $h = 0.8\mu\text{m}$. It can be seen that the width of the protrusion

of the surface structure and the region of the film under it a periodic alternation of red-white-blue colors is observed, which corresponds to phase change by 2π and can be interpreted as a certain dimensional resonance of spin waves with a length of about fractions of micron. We assume that such short waves can be experimentally excited using a wide microstrip (although not very efficiently) according to the mechanism proposed in [26].

4. Possibility of practical application

Note that dependence $f^*(H)$, close to the linear one, can serve as an advantage for practical application similar to the use of magnonic crystals for the development of magnetic field sensors [13–17]. The matter is that in the case of MC the dependence on H of the central frequency of the Bragg stopband f_B linked, for example, for SMSW, with the SW wavenumber k by the dispersion relation (1), is controlled. For example, in Fig. 2, a the curve 2 corresponds to the dependence of the frequency of the first Bragg resonance f_B in a film with the chosen parameters and grating period $\Lambda = 100 \mu\text{m}$. It can be seen that for the fixed value k the dependence $f_B(H)$ differs significantly from the linear one in the region of low magnetic fields.

5. Conclusion

In the frequency dependence of the power reflected from a microstrip antenna, on which a film of yttrium iron garnet with metasurface is located, a narrow region of the reflected power decreasing was found, the central frequency of which linearly depends on the magnitude of the bias field H in the range from several Oe to 1.7 kOe. This dependence can be useful for the development of magnetic field sensors. The results of the measurements are in qualitative agreement with the results of micromagnetic modeling, which allow us to interpret the detected feature in the reflected power as a result of dimensional resonances of spin waves in the metasurface elements.

Funding

This study was carried out within the framework of a state assignment and partially supported by the Russian Foundation for Basic Research (RFBR projects No. 20-07-00973, No. 20-57-00008 and No. 20-07-00968).

Conflict of interest

The authors declare that they have no conflict of interest.

References

- [1] J.O. Vasseur, L. Dobrzynski, B. Djafari-Rouhani, H. Pushkarski. *Phys. Rev. B* **54**, 1043 (1996).
- [2] M. Krawczyk, H. Puzkarski. *Acta Phys. Pol. A* **93**, 805 (1998).
- [3] M. Krawczyk, H. Puzkarski. *Phys. Rev. B* **77**, 054437-12 (2008).
- [4] V.V. Kruglyak, A.N. Kuchko. *Physics B* **339**, 130 (2003).
- [5] V.V. Kruglyak, A.N. Kuchko, V.I. Finokhin. *FTT* **46**, 842 (2004) (in Russian).
- [6] V.S. Tkachenko, V.V. Kruglyak, A.N. Kuchko. *J. Magn. Magn. Mater.* **307**, 48 (2006).
- [7] H. Pushkarski, M. Krawczyk, J.-C. S. Levy. *J. Appl. Phys.* **101**, 024326 (2007).
- [8] A.N. Kuchko, M.L. Sokolovsky, V.V. Kruglyak. *FMM* **101**, 565 (2006) (in Russian).
- [9] S. Neusser, D. Grundler. *Adv. Mater.* **21**, 1 (2009).
- [10] A.A. Serga, A.V. Chumak, B. Hillebrands. *J.Phys. D* **43**, 264002 (2010).
- [11] A.V. Ustinov, A.V. Drozdovskii, B.A. Kalinikos. *J. Appl. Phys.* **96**, 142513 (2010).
- [12] M. Krawczyk, D. Grundler. *J. Phys.: Condens. Matter.* **26**, 12, 123202 (2014).
- [13] M. Inoue, A. Baryshev, H. Takagi, P.B. Lim, K. Hatafuku, J. Noda, K. Togo. *Appl. Phys. Lett.* **98**, 132511 (2011).
- [14] R.G. Kryshal, A.V. Medved. *Appl. Phys. Lett.* **100**, 192410 (2012).
- [15] P. Talbot, A. Fessant, J. Gieraltowski. *Proc. Eng.* **120**, 1241 (2015).
- [16] S. Atalay, A.O. Kaya, V.S. Kolat, H. Gencer, T. Izgi. *J. Supercond. Nov. Magn.* **28**, 2071 (2015).
- [17] H. Takagi, J. Noda, T. Ueno, N. Kanazawa, Y. Nakamura, M. Inoue. *Electron. Commun. Jpn* **97**, 11 (2014).
- [18] R.L. Carter, C.V. Smith, J.M. Owens. *IEEE Trans. Magn. MAG-16*, 1159 (1980).
- [19] Yu.V. Gulyaev, S.A. Nikitov, L.V. Zhivotovsky, A.A. Klimov, Ch. Tsai, F. Tayed, S.L. Vysotsky, Yu.A. Filimonov. *Pis'ma v ZhETF* **77**, 670 (2003) (in Russian).
- [20] S.L. Vysotskii, Y.V. Khivintsev, V.K. Sakharov, G.M. Dudko, A.V. Kozhevnikov, S.A. Nikitov, N.N. Novitskii, A.I. Stognij, Y.A. Filimonov. *IEEE Magn. Lett.* **8**, 3706104 (2017).
- [21] S. Vysotskii, G. Dudko, V. Sakharov, Y. Khivintsev, Y. Filimonov, N. Novitskii, A. Stognij, S. Nikitov. *Acta Phys. Pol. A* **133**, 508 (2018).
- [22] S.L. Vysotsky, S.A. Nikitov, Yu.A. Filimonov, E.S. Pavlov. *Radiotekhnika i elektronika*, **55**, 855 (2010) (in Russian).
- [23] A.G. Gurevich, G.A. Melkov. *Magnitnye kolebaniya i volny. Fizmatlit, M.* (1994). 464 s. (in Russian).
- [24] M. Donahue, D. Porter. *OOMMF User's Guide, Version 1.0.Ed. In Interagency Report NISTIR 6376. Boulder: Nat. Inst. of Standards and Technology.* (1999).
- [25] M. Dvornik. *Magnonics: from fundamentals to applications. Ch.: Micromagnetic Simulations in Magnonics / Eds M. Dvornik, Y. Au, V.V. Kruglyak. Springer-Verlag, Berlin Heidelberg* **125**, 101 (2013).
- [26] Haiming Yu, G. Duerr, R. Huber, M. Bahr, T. Schwarze, F. Brandl, D. Grundler. *Nature Commun.* **4**, 2702 (2013).
- [27] R.W. Damon, J.R. Eshbach. *J. Phys. Chem. Solids.* **19**, 30 (1961).